Valuing Solar Subsidies

Bryan Bollinger* Kenneth Gillingham† A. Justin Kirkpatrick‡

January 20, 2023

Abstract

Individuals trade future for present consumption across a range of economic behaviors, and this tradeoff may differ across demographics. This study employs unique data on rooftop solar adoption and the expected returns from such adoption to estimate heterogeneous discount rates by wealth. We develop a dynamic discrete choice model of optimal system sizing and adoption, and base identification on plausibly exogenous variation in the future savings from installing solar and electricity rates. We estimate implied discount rates of 19.8%, 10.3%, and 10.8% for low-, medium-, and high-wealth households in California. Counterfactual simulations demonstrate opportunities to reduce the regressivity of solar adoption and improve policy cost-effectiveness.

Keywords: solar, discount rates, energy policy, distributional impact

*New York University
†Yale University and NBER
‡Michigan State University. Email: jkirk@msu.edu

1 Introduction

The rate at which individuals trade future consumption for present consumption is important across a range of economic behaviors, including savings, human capital formation, health maintenance, etc. It is also important for public policy, particularly amid claims that welfare of sometimes irrational consumers can be enhanced by reduced consumer choice, e.g., with respect to energy-consuming durable goods. Energy-efficiency standards for autos and household appliances, for instance, are credited with cost savings to consumers whose choices imply sufficiently high discounting of future energy costs that they are attributed to optimization mistakes. Laboratory experiments on intertemporal decision-making are numerous, but credible quasi-experimental estimates of discount rates revealed by market decisions are relatively scarce, e.g. Hausmann 1979, Warner and Pleeter 2001, Allcott and Wozny 2014. Evidence on how discount rates vary demographically for relevant populations is even scarcer.

This paper, therefore, employs rich and unique micro-data on rooftop solar panel adoption and on the rooftop expected returns from solar panel adoption to estimate heterogeneous discount rates as they depend on household wealth. Solar purchases entail an upfront cost to install panels that generate future electricity cost savings as a function of the sunlight that falls upon the panels and the retail electricity rates at which solar generation is compensated in California and many other states. Thus, using proprietary Google Sunroof data, we observe the rooftop-specific expected electricity generation of optimal solar installations for every home in select California counties. We also observe the adoption decisions of these households in data provided by the Lawrence Berkeley National Laboratory. We use these data, combined with household electricity consumption data from a California utility and household-specific wealth, income and other demographic information from InfoUSA, to develop a structural solar adoption model that estimates household preferences for flows of benefits, accounting for optimal installation size and household consumption. Discount rates are identified from plausibly exogenous variation in future savings due to rooftop characteristics, such as pitch, orientation, and shading from trees and structures, and from discrete differences in electricity rates across administratively determined climate zones within the state.

We consider how households trade off upfront solar PV system costs and future savings on grid electricity by exploiting both discrete changes in future energy savings across administrative borders, and plausibly exogenous variation in household system costs resulting from exogenous variation in roof exposure, orientation, and shading. In doing so, we evaluate the efficiency of upfront capacity incentives that include a federal investment tax credit and state and local rebates relative to net energy metering (NEM) policies common to 43 U.S. states; NEM policies subsidize a future stream of electricity generated over the 20-25-year lifetimes of solar PV systems by requiring utility companies to roll back a household's meter by the generated solar electricity, in effect requiring the utility to purchase the solar electricity at the retail rate. However, this stream of economic benefits may be highly discounted by impatient households who are observed to under-invest in energy-saving durables in a phenomenon termed the "Energy Paradox" that is believed to yield an "Energy Efficiency Gap" (Hausman 1979; Dubin and McFadden 1984; Li et al. 2009; Bento et al. 2012; Allcott and Wozny 2014). If households exhibit discount rates higher than market rates, then policymakers interested in increasing solar electricity generation could redeploy public resources embodied in NEM policies in the form of upfront capacity rebates or expected generation rebates that effectively arbitrage household impatience.

We estimate statistically significant and economically meaningful differences in discount rates between low- and high-wealth homeowners. The decline in rates with wealth is consistent with theories of credit constraints that bind more for low-income than high-income households. Because solar panels produce a homogeneous input into utility, electricity, and because the intertemporal tradeoff of upfront costs for future cost savings is the dominant characteristic of the adoption decision (as opposed to comfort, safety, noise, size, brand, etc.), these estimates are likely unbiased by correlated unobservables or consumer inattention. Hence, they provide credible evidence that individual discount rates exceed market rates and that these vary by wealth in ways that have important implications for policy. First, these discount rates imply a smaller role for the energy paradox in explaining consumer decisions. Second, they indicate that current state net-energy-metering policies that subsidize future solar electricity generation could arbitrage differences in individual and market discount rates to increase solar adoptions per unit expenditure by offering upfront rather than future subsidies. Thirdly, our results suggest the current subsidy policies common to most states yield greater utility to high-income households than low-income households due to heterogeneous discount rates, highlighting a structural inequity in existing solar policy.

Despite the prevalence of NEM policies and the vigorousness with which they are defended, we are not aware of any previous research that has evaluated their effectiveness across wealth levels in spurring additional solar PV capacity or generation. Upfront rebates and financing mechanisms, on the other hand, have been studied by Kirkpatrick and Bennear (2014), Hughes and Podolefsky (2015), Rogers and Sexton (2015), Gillingham and Tsvetanov (2017) and Pless and van Benthem (2016). NEM policies have proven controversial because they are believed to shift costs from relatively wealthy households who preferentially adopt rooftop solar to relatively poor households who do not. Solar adopters avoid paying for fixed costs of grid investment and maintenance that are commonly incorporated into the volumetric charges of retail tariffs. Such cost-shifting is of concern to regulators for equity reasons alone. Also of concern, however, is the viability of traditional utility models if NEM policies are unreformed. As fixed costs are spread across smaller retail electricity sales, rates are likely to rise, inducing further grid defections that could yield a "utility death spiral" (Kind 2013).[1]

2 Background

Existing rooftop solar subsidy regimes have generated additional solar capacity and generation at relatively high cost partly due to take-up by infra-marginal adopters, i.e., free-riders who would have adopted solar in the absence of subsidies (Hughes and Podolefsky 2015; Gillingham and Tsvetanov 2014; Rogers and Sexton 2015. Moreover, the additional capacity may not be sited to yield maximum generation let alone maximum value of generation. Finally, as Borenstein and Davis (2016) show, the subsidy benefits accrue mostly to wealthy households who preferentially adopt solar, raising concerns about the distributional impacts of state and federal incentives for solar capacity and generation. This project considers opportunities for improving the efficiency and equity of existing solar policy.

[1]We distinguish a subsidy mechanism from the funding sources in order to study the cost-effectiveness of NEM subsidies, i.e., the public cost per additional unit capacity or additional unit generation. Welfare analysis that accounts for transfers from some electric utility customers to solar adopters, as is customary in existing NEM policies, is beyond the scope of this paper. However, our interest in this research question centers on the potential for a policy innovation that spurs greater solar adoption without the cost-shifting that hinders utility fixed cost recovery and distributional objectives.

Typically, a subsidy on the extensive (adoption) margin would sacrifice efficiency on the intensive (generation) margin. However, the feedstock for solar electricity generation is free, and so marginal costs of generation are negligible. Indeed, industry groups advise that rooftop systems don't even require any routine maintenance.[2] Moreover, our own preliminary analysis of monthly generation from rooftop systems receiving a California generation subsidy or an upfront subsidy for expected generation exhibit no output degradation over their lifetimes and no differential effects across subsidy mechanisms of system age.[3] Therefore, the decision to adopt solar is made as a "set it and forget it" decision requiring only consideration of up-front investment and the (constant) flow benefits.

Solar net metering acts as a flow or production subsidy by reducing a customer's electricity bill by more than the value of the electricity generated. This is due to the true-up period used in most net metering policies. A solar household may generate more electricity than is consumed during sunny afternoons, and the excess energy is injected into the grid. Increasingly, the wholesale value of that injection is low – when residential rooftop solar panels are producing at a high rate, so too are utility scale solar installations, which lowers the wholesale price of electricity that determines the value of the residential injection. Under net metering, this injected energy is credited against subsequent withdrawals from the grid, even when those withdrawals occur at high wholesale cost time periods, such as evenings just after sunset. The "wedge" can be in excess of \$0.20/kWh. In effect, this is a subsidy for solar adopters with NEM.

Solar panels generate electricity for more than 20 to 25 years, and NEM policies are generally "locked in" (though exceptions to this exist). Therefore, the net present value of the flow of subsidies varies greatly with the household's discount rate. This net present value of solar is the main comparison a household makes when weighing substantial up-front investment costs with the benefits of "going solar". Therefore, the key economic element in household solar decisions necessary to understand uptake, in addition to levels of flow payoffs and levels of net up-front costs, is the household discount rate. This paper empirically estimates these discount rates.

Notably, California has recently begun the process to amend its net metering policy to address the regressivity of the existing net metering policy. In November 2022, an administrative law judge in California issued a draft proposal for revisions to California's NEM policy as required under AB327 (2013). Previously, the California Public Utilities Commission (CPUC) had developed a set of priorities for net metering revision, in accordance with existing law, that emphasized, *inter alia*, that net metering payouts made to rooftop solar must reflect the *avoided cost* of generation based on the location and time of injection into the grid. Furthermore, the priorities sought to emphasize equity of burden as previous look-back studies had found that low-income households bore a large burden of fixed costs imposed by previous net metering programs 1.0 and 2.0 (Hymes, 2022). In December 2022, the CPUC voted unanimously to adopt this proposed "Net Metering 3.0" plan which would drastically decrease the payout for rooftop generation net of consumption and would provide an income-based glide-path of supplemental payments to encourage adoption of rooftop solar for a term of five to nine years. The

[2] See for instance https://www.energysage.com/solar/101/solar-panel-maintenance/.

[3] Aldy et al. (2017) estimate that wind farms choosing to receive a federal capital subsidy produce 8-13% less electricity per unit of capacity than wind farms selecting to receive a federal output subsidy, and that this effect is driven by incentives generated by these subsidies rather than selection. Like solar generation, the feedstock for wind generation is free. However, there are more operating margins for wind than for solar. Turbines, for instance, can be damaged by weather if they are spinning (and generating) in very high wind conditions.

need for reform has brought the issues of net metering, in particular the distribution of wealth amongst households that benefit. Counterfactuals in Section 7.2 are aimed at understanding the effects of some of the proposed reforms.

3 Data

Our main dataset is comprised of household-level data from six sources: CoreLogic, which provides property and house characteristics acquired from county recorders and assessors; Lawrence Berkeley National Laboratory's *Track The Sun* proprietary address-level dataset of all known solar installations; Google Project Sunroof, which provides house-level solar irradiance profiles; InfoUSA, which provides household demographics including wealth and income; Pacific Gas and Electric household consumption data; and the California Secretary of State's voter registration database, which provides address-level voter registration.

3.1 Data Description

3.1.1 Sample Selection

We assemble the study sample by first identifying zip codes in California that are located within the Pacific Gas and Electric service territory. For a subset of these zipcodes described below, we extract from CoreLogic all single-family detached non-mobile home residences built before 2014 that are owner-occupied using CoreLogic's owner-occupancy flag. House data includes the year built, heated square footage, and the number of stories.

3.1.2 CEC Climate Zone Boundaries

Our identification strategy relies, in part, on leveraging differences in electricity prices across California Electric Commission (CEC) climate zones. We identify the climate zone associated with each zip code in the Pacific Gas and Electric service territory and extract from the sample home in those zip codes that lie on a climate zone boundary[4]. The 28 zip codes contained in the sample are shown in Figure 1.

While all households in the PGE service territory share the same block pricing steps at any given time, CEC climate zones vary in the *width* of a block tier pricing step – hotter inland zones are allowed more baseline consumption before stepping up to the next higher marginal rate relative to cooler coastal zip codes. Our sample includes homes in 28 zip codes that are wholly contained in one of three unique CEC climate zones (PG&E territories S, T, and X). While all homes initially face the same price per kilowatt-hour for their first unit of consumption, homes in warmer CEC climate zones will, as consumption increases, face lower retail rates than will homes in cooler CEC climate zones due to the higher threshold for stepping to the next block tier price. Average retail price per kilowatt-hour is weakly lower in warmer CEC climate zones with higher baseline thresholds. During the study period, baseline thresholds were adjusted once. Thresholds are shown over time in Figure 2. The sample contains 34,796 households in zip codes in Territory S, 57,790 households in zip codes in Territory T, and 91,081 households in zip codes in Territory X.

[4]During the study period, PG&E designated CEC climate zones as "baseline territories". We use PG&E published rates by territory, but note that these territories follow the CEC climate zone boundaries.

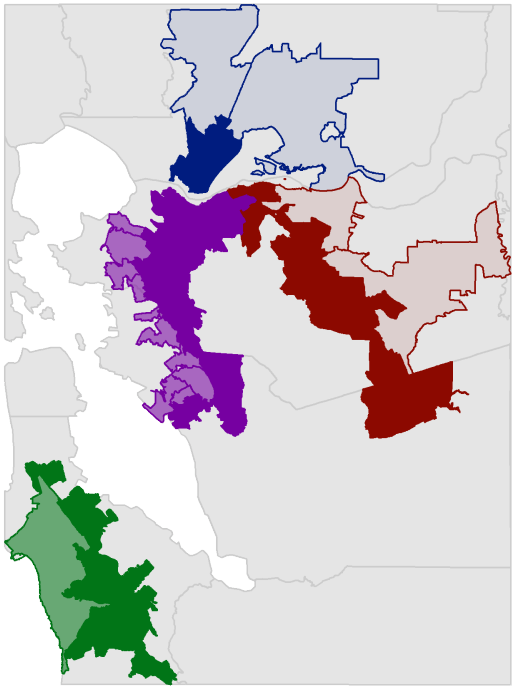


Figure 1: **Sample zip codes**. Zip codes in PG&E service territory that share a CEC climate zone boundary. Climate zones determine baseline allowances used to determine block pricing step "width". Zip codes along a boundary face different average value of offset electricity when moving across the boundary. Color indicates boundary-spanning groups.

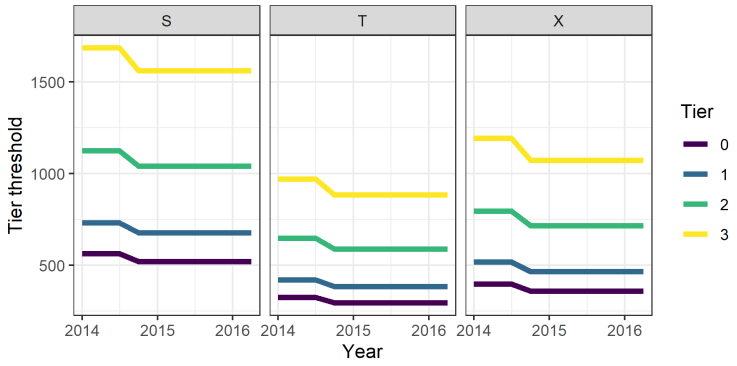


Figure 2: **Rate tier climate zone thresholds**. CEC climate zone thresholds over time in kilowatt-hours per month. Corresponding rates are shown in Figure 3

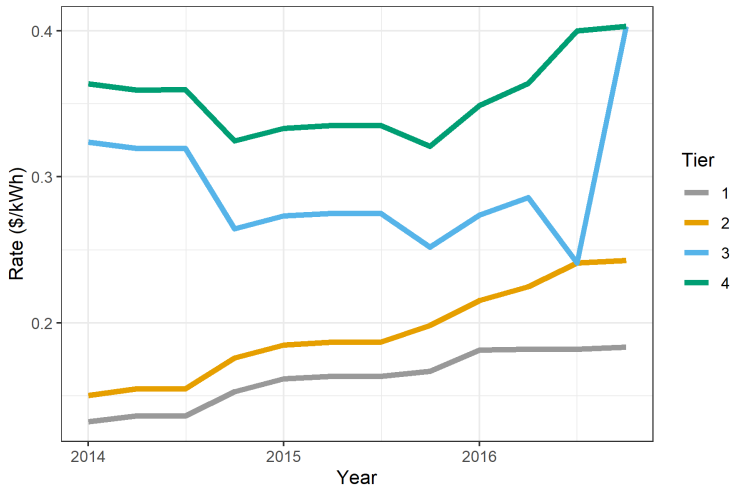


Figure 3: **Retail Rates**. Retail rates by tier over time in dollars per kilowatt-hour.

In addition to spatial CEC climate zone variation in block tier step width, retail electricity rates for each step of block tier pricing vary over time.

3.1.3 Household Characteristics

We merge publicly-available household voter affiliation provided by the California Secretary of State which indicate the voter affiliation of each person in the State. We match on address and generate a voter affiliation of the household by taking the affiliation of the two oldest registrations at an address that voted in the 2014 elections. We identify the household as registered Democratic if and only if all of the two longest-registered 2014 voters are registered Democrats or are registered with the Green Party.

Data from InfoUSA include the number of children, the length of time at the residence, the head of household's age and ethnicity, the number of open lines of credit, and the calculated wealth of the household. We merge by address and take only the individuals present from 2014-2016. If the address has more than one household we use the data from the household that occupied the home for the plurality of our study period.

Table 1 shows summary statistics for the homes and households in the sample by adopter status. Adopters tend to be middle- and high-wealth, are more likely to have children, and have larger homes. White households are over-represented among adopters, while Black, Asian, and Hispanic households are under-represented.

3.1.4 Household Irradiance Profiles

Each household faces an optimal installation size that depends on their initial electricity consumption, as well as the cost of installing solar. Homes located in deep shade or with a roof profile that does not angle southward need more panels to generate a given amount of electricity, increasing the cost per kWh to that household. This is our main source of identifying variation. We match each household in our data to the nearest Google Project Sunroof record with a greedy spatial matching algorithm. We

Table 1: Summary Statistics

			Adopters			Non-adopters		
		Pct. Sample	Mean	Std. dev	Pct. of Type	Mean	Std. dev	Pct. of Type
	Wealth	100.00	2654.65	945.81		2567.56	1055.69	
	Lines of credit	100.00	0.75	1.53		0.66	1.40	
	Children present	100.00	0.41	0.49		0.32	0.47	
	Length of residence	100.00	13.62	10.71		15.77	12.39	
	Square Footage	100.00	2.13	0.82		1.78	0.75	
Stories	1	69.38			57.54			69.98
	2+	30.62			42.46			30.02
Age	¡40	16.58			16.99			16.56
	40-64	55.86			60.28			55.63
	65+	27.56			22.74			27.81
Ethnicity	Asian	10.31			8.99			10.38
	Black and Other	12.76			10.74			12.86
	Hispanic	15.90			14.84			15.95
	White	61.03			65.42			60.81
Voter affiliation (D)	Dem	41.90			45.23			41.74
	Rep, Mixed, or Unaffiliated	58.10			54.77			58.26
Wealth Bins	High	31.13			30.13			31.18
	Low	34.40			27.82			34.73
	Med	34.47			42.05			34.09

drop the 5% of households with the largest distance between the geocoded home address and the Google Sunroof record.

Figure 4 shows an example of the Google Project Sunroof website which shows the irradiance profile of two homes, one with a sunny, unobstructed, south-facing roof, and the other with low irradiance and no substantial south-facing roof. These homes are located in the same neighborhood in East Lansing, Michigan, and are served by the same electric utility.

For each matched household, our data contains the panel-by-panel expected generation. Generation is largely decreasing as panels are ordered by generation, though contiguity requirements may result in some increases. Figure 5 shows six randomly selected rooftops' generation profile.

3.1.5 Household Consumption Profiles

From Pacific Gas and Electric (PG&E), we obtain confidential customer annual consumption for all customers in any of the 28 zip codes in the sample. Data is anonymized and does not include address beyond the 5-digit zip code, but does include grid interconnection IDs that identify solar adopters. Thus, for solar adopters, we observe the annual consumption prior to the installation of solar and can designate the closest consumption bin for each adopter. For non-adopters, we see only the full distribution of consumption across the zip code. For each zip code, we remove known adopters and bin all consumption into five equal-sized consumption bins. We calculate the mean consumption for each bin within each zip code. The study period is relatively short (8 or 10 quarters), so we treat consumption as fixed over the study period. A density plot of zip-level consumption is shown in Figure 6.

Figure 7 shows the consumption levels of adopters and non-adopters by wealth. Across all three weath bins, adopters have higher consumption on average. As wealth increases from low- to medium, the separation between average consumption of non-adopters and average consumption of adopters becomes larger, consistent with lower discount rates and higher sensitivity to the flow of benefits from installing solar



Figure 4: **Google Project Sunroof display.**(Top) shows example readout for the home marked with location flag. This home enjoys unobstructed sunlight and has a large, flat, south-facing roof segment. Google Sunroof predicts substantial savings when installing solar on this home. (Bottom) this home has extensive shading and does not have a substantial south-facing roof segment. Google Sunroof predicts lower savings when installing solar on this home. These homes are in the same neighborhood in East Lansing, Michigan, and are served by the same electric utility.

3.2 Model Free Evidence

Payoffs to adopting solar take the form of offset grid consumption, expressed as the discounted sum of $q^*\bar{p}$, where q^* is the optimal annual generation and $\bar{p}$ is the average per-kWh price of electricity for those units offset by an solar installation. Households that offset more electricity (higher q^*) or more valuable electricity (higher rates due to higher consumption, rate structure, or time variation in rates) are more likely to adopt solar. Furthermore, because these benefits occur in the flow payoff – savings over the life of the installation – households with lower discount rates will be *more* responsive to higher q^* or higher $\bar{p}$.

Rooftop irradiance provides plausibly exogenous variation in q^* allowing us to identify discount rates from variation in responses to $q^*\bar{p}$. The structural model in Section 4 formalizes the use of this variation, but here we provide model-free evidence of this relationship. Figure 8 shows the share of observed adopters in the sample by quantiles of irradiance. We measure irradiance in three ways - the generation of the first panel, the rate of decline for each additional panel, and finally the total generation from a 15-panel array which can be thought of as a reasonable composite of the first two. Figure 8 shows the two main relationships. First, adopting shares increase over all income levels when irradiance increases. Second, the rate of increase is higher for medium- and high-wealth households relative to the Low wealth households. This indicates wealth-based differential response to increases in the flow payoff of solar. If low-wealth households are less responsive to increases in the flow payoffs, then low-wealth households put less value on payoffs that occur in the future relative to the present.

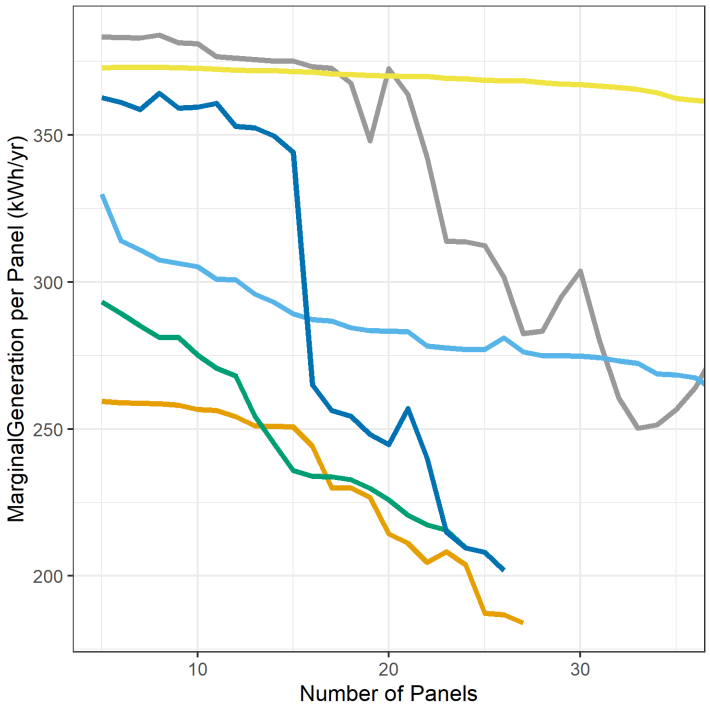


Figure 5: **Irradiance profiles** for six randomly selected rooftops. Figure shows marginal generation for each household on vertical axis per panel on horizontal axis. Contrast Orange, which exhibits low irradiance (260 kWh/yr) for the first panel and a slow decline up to 15 panels followed by a rapid decline, with Gray, which exhibits strong irradiance for the first 20 panels (340 kWh/yr) followed by a rapid decline.

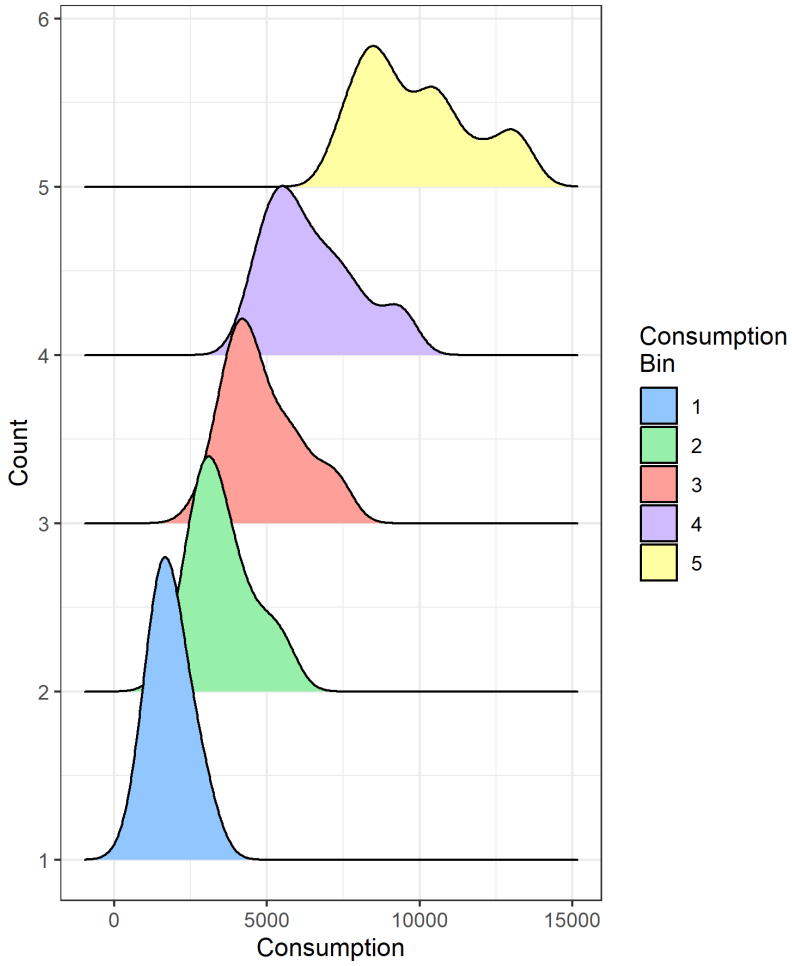


Figure 6: **Distribution of zip-level consumption bins** calculated from the full distribution of consumption by zip code. For each zip code, consumption is grouped into one of five bins (1 is lowest consumption, 5 is highest) and the mean consumption is calculated for each bin. Plot shows the distribution across zip codes of the five bin's mean consumption.

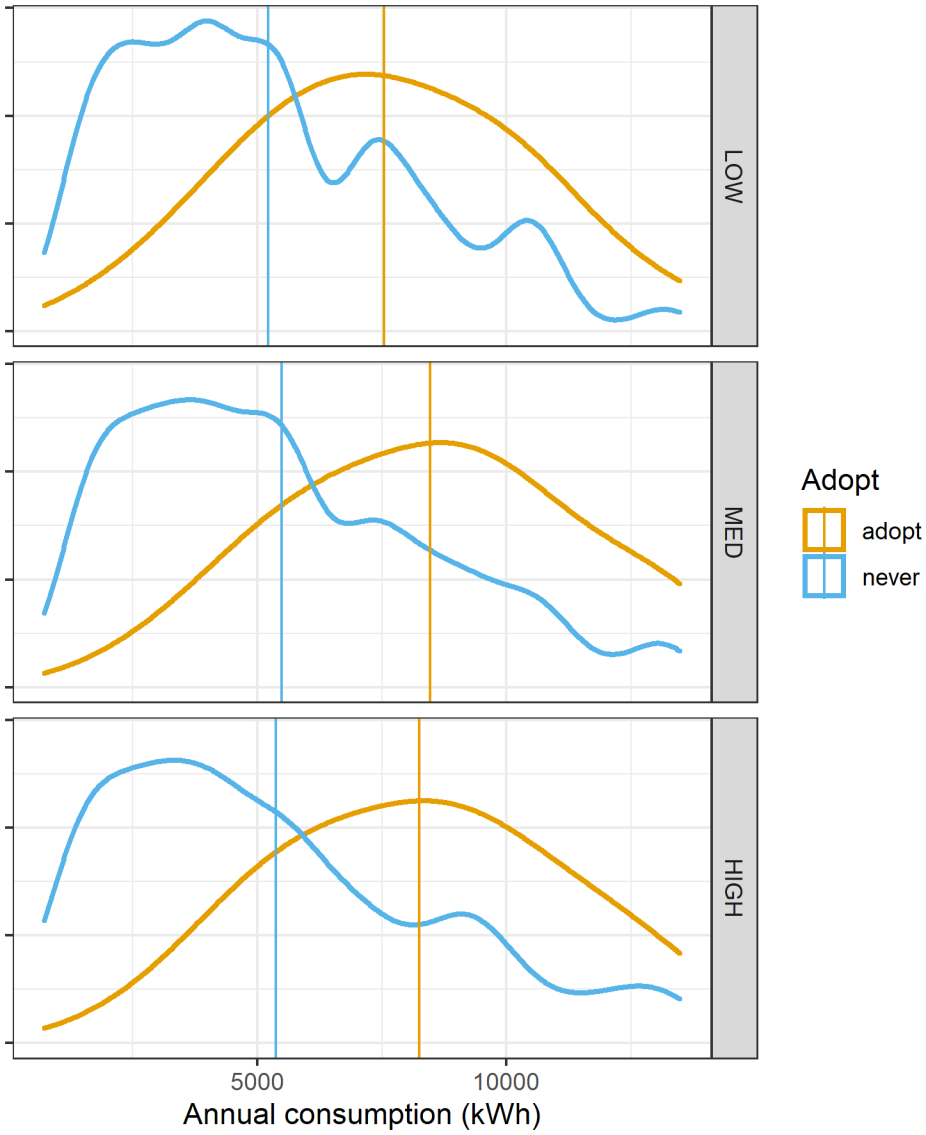


Figure 7: Density of consumption by adopter status and wealth. To calculate density of non-adopters, we assign equal weight to each of the five consumption bins for the household's zip code.

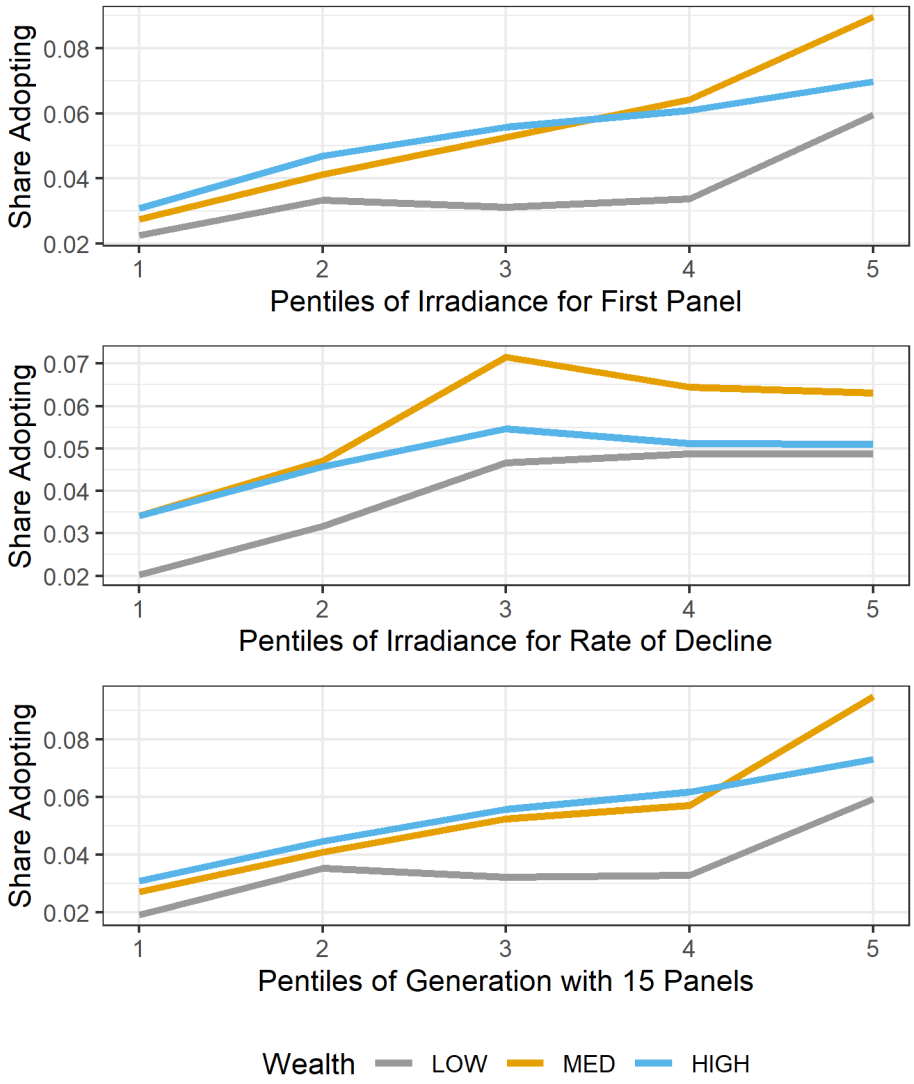


Figure 8: Observed share adopting over quantiles of measures of irradiance by wealth. (Top) shows the change in observed share adopting as first panel irradiance increases. (Middle) shows the change in observed share adopting as roof profile rate of decline decreases (higher generation read left-to-right).(Bottom) the change in observed share adopting as total generation at 15 panels increases. High and Medium wealth households respond more to irradiance than does the Low wealth bin, evidenced by the more positive slope for High and Medium.

Households with higher irradiance have either higher payoffs from adopting solar due to larger optimal size installations offsetting higher levels of consumption, *or* face lower total up-front cost due to smaller sized installations. To isolate the effect of $q^*\bar{p}$ on adoption by wealth, we may take a cross-sectional approach. In Figure 9, we restrict a sample to only those households with an optimal installation cost within a window around the mean total cost in the data. With the cost term fixed, we examine the cross-sectional variation in terciles of $q^*\bar{p}$, the flow payoff of installing, and the share observed to adopt. Variation in $q^*\bar{p}$ is the result of differences in rooftop irradiance, electricity rates, and consumption. Figure 9 shows two results. First, conditional on a fixed total cost, higher values of $q^*\bar{p}$ result in higher shares of adoption in the data. Second, high-wealth and medium-wealth households respond more positively to increases in $q^*\bar{p}$ than do low-wealth households. A more positive relationship between $q^*\bar{p}$ and share adopting indicates higher valuation of a fixed flow, which indicates a lower discount rate.

4 Model

4.1 Sizing

The decision to adopt solar depends upon a determination of the optimal system size conditional on adoption, and then a comparison of average electricity costs with and without solar adoption. The optimal size of the system is a function of system costs and upfront capacity rebates, the marginal cost of grid electricity, and system generation, which is a function of capacity and the effective solar irradiance of each portion of the optimal solar array. Effective solar irradiance is a function of the amount of sunlight that falls to the earth at the location of adoption. This irradiance varies considerably across the U.S. and around the world, and even within U.S. states, e.g., across zip codes. It is modeled from satellite imagery and is also a function of climate. The National Renewable Energy Laboratory models irradiance at the 10-square kilometer level. This irradiance, therefore, does not vary at the very local level. Effective irradiance, however, also accounts for the obstruction of some solar irradiance by surrounding structures and vegetation, as well as panel orientations and pitches that may fail to capture all irradiance due to rooftop characteristics. Effective irradiance, thus, admits micro-level variation in the electricity generation of a unit of solar capacity, namely from household to household within neighborhoods, Moreover, for a given home, effective irradiance varies across the rooftop, with some portions of the rooftop receiving more sunlight than others.

Solar panel installation is characterized by economies of scale. This is true both for utility-scale and rooftop installations (Barbose et al. 2013). In both contexts, there are fixed costs associated with modeling the installation site to optimize size, orientation, and equipment, as well as obtaining permits and relevant regulatory approvals. These fixed costs cause the average cost of solar electricity to decline in system size, all else equal. Hence, utility-scale systems tend to be cheaper than rooftop systems, and the cost per watt of large rooftop systems is lower than the per capacity cost of small systems. However, because effective irradiance is non-increasing in system size and commonly decreasing in size, average solar electricity costs likely decrease over a range of rooftop capacity before increasing until rooftop surface areas is exhausted.

Let $TC(K)$ denote the total cost to a household of a solar installation of size K. It is comprised of a fixed cost, F and a cost per panel, V. The panel cost is reduced by available per-capacity subsidy,

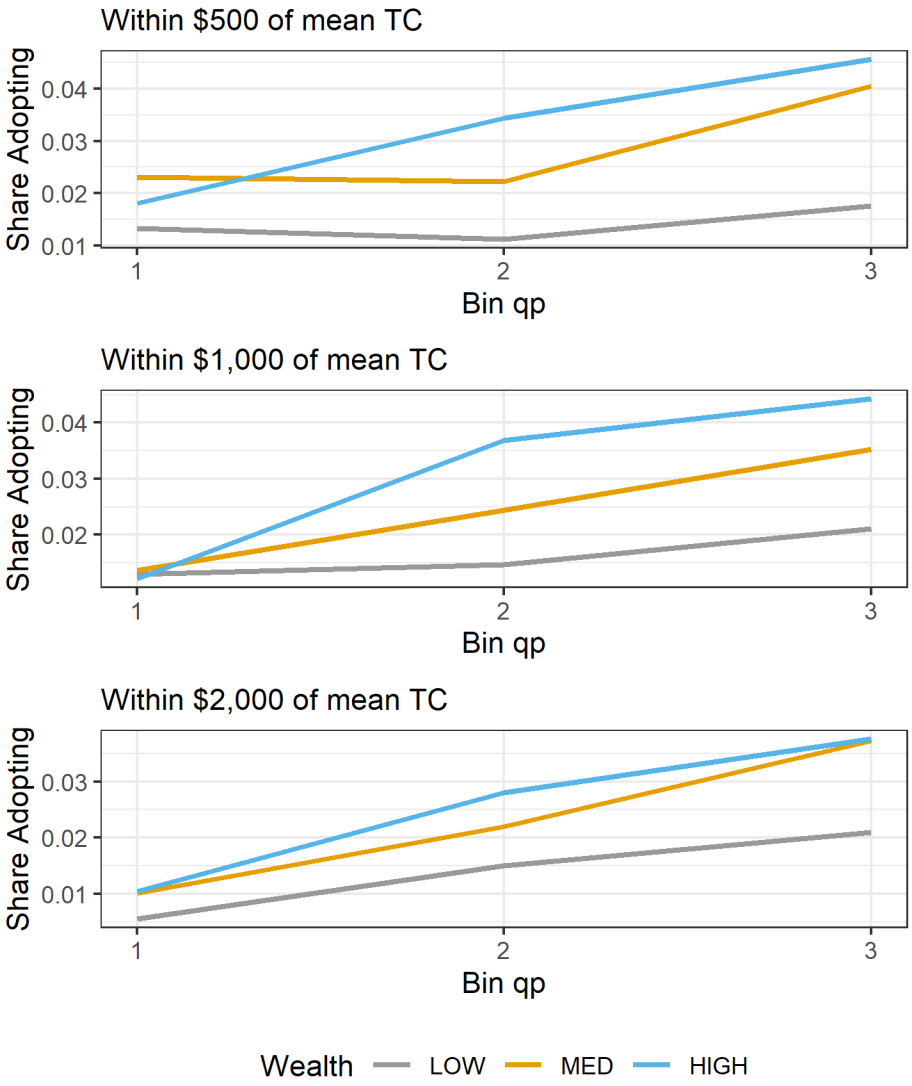


Figure 9: **Adoption rates by wealth holding total cost fixed.** Each panel shows the adoption rate across wealth bins for flow payoffs in each of three terciles along the x-axis, holding the system total cost fixed within a band around the mean. Holding up-front total cost fixed, variation in the flow payoff $q^*\bar{p}$ (labeled as qp) results from electricity rates and optimal size differences. In nearly all cases, high- and medium-wealth households adopt at a higher rate (orange and blue are above gray). As the flow payoff increases, adoption rates rise, but the rate of increase is largest for high- and medium-wealth households. This is consistent with variation in discount rates where high- and medium-wealth households have lower discount rates relative to low-wealth households. This illustrates the source of identification of discount rates by wealth.

S. The total cost of the system net of rebates is reduced by a fraction I equal to the investment tax credit.[5] Thus,

$$TC(K) = (F + K \cdot (V - S))\,(1 - I)$$

Define $C = (V - S)(1 - I)$ as the constant marginal system cost (or cost per unit of capacity).

Let $q(K)$ be the annual electricity generated by a system of size K (and q^* is the annual electricity produced by a system of optimal size K^*). Then $q'(K)$ is marginal generation, i.e., the electricity produced by an incremental unit capacity. We assume $q'(K)$ is weakly decreasing in K because the first unit of solar capacity is installed on the highest solar irradiance surface of a rooftop, i.e., $q'(K) \geq 0, q''(K) \leq 0$. The cost per kWh of electricity generated by the marginal unit of capacity over its (25-year) lifetime, $c(K)$, is then equal to $(V - S)(1 - I)/25q' = C/25q'$. An interior solution to the sizing problem equates the present value of the levelized cost of electricity generated by the marginal unit capacity to the present value of the 25-year future stream of utility payments for the marginal unit of consumption from the grid.[6] Assuming annual discounting at a rate δ, the present value cost of the marginal unit of grid electricity consumption over the lifetime of the solar capacity is $\sum_{t=1}^{25} \frac{1}{(1+\delta)^t} p$, where p is the annual cost of the monthly marginal unit of electricity consumption. Thus, the optimal system size (in an interior solution to the first order condition) is implicitly defined by:

$$c(K) = \sum_{t=1}^{25} \frac{1}{(1+\delta)^{t-1}} p,$$

where $c(K)$ is increasing in K because q' is decreasing in K. Because q' is decreasing in K, for constant and increasing block rate prices, there will be a unique optimum. With increasing block prices, the first units of displaced grid electricity bear the highest marginal costs, and marginal costs of displaced electricity decline discretely as solar capacity increases. For decreasing block prices, the opposite is true, and the interior optimum may not be unique. Optimal size is increasing in q', p, S, and I and decreasing in δ and V.

The optimal sizing of a system is a function of the NEM policy regime. Here we assume an NEM policy whereby rooftop system generation is compensated equivalently whether it is consumed in the household, thereby displacing grid imports, or whether it is exported to the grid, i.e., the NEM is equal to the retail rate. This assumption is consistent with the vast majority of NEM policies in effect in the U.S. Were exports not compensated at as great a rate as on-site consumption, or perhaps not compensated at all, then the optimal sizing decision would be different. In particular, optimal sizes would be smaller. Because most NEM policies restrict compensation for exports to annual or monthly quantities less than or equal to total consumption less on-site consumption of solar generation, households will not install solar capacity greater than that which is sufficient to fully offset electricity consumption.

The optimal sizing function is piece-wise defined according to the number of tiers in the tariff structure. We illustrate this in the context of a tariff with two distinct tiers of volumetric charges. We abstract from consideration of fixed charges because we assume no households prefer to disconnect from the grid. Let τ be the monthly grid consumption threshold at which rates change from p_0 to p_1 for

[5]This assumes federal income tax liability. The absence of tax liability is a likely reason why low-income populations are less likely to adopt rooftop solar. For the empirical methods that follow, this modeling assumption is not important.

[6]We assume households take electricity consumption as given and seek the minimize the cost of that consumption.

$p_0 < p_1$, and let q_0 denote monthly household consumption. The marginal price of grid electricity p depends upon the residual grid demand, i.e., consumption net of solar generation, such that:

$$p = \begin{cases} 0 & q_0 - q \leq 0 \\ p_0 & 0 < q_0 - q < \tau \\ p_1 & q_0 - q \geq \tau \end{cases}.$$

The piece-wise-defined solution to the optimal sizing problem for increasing block rates and a household consuming at the highest rate, is defined as:

$$K^* = \begin{cases} 0 & c(0) > p_1 \\ (q')^{-1}\left(\frac{C/25}{\sum_{t=1}^{25}\frac{1}{(1+\delta)^t}p_1}\right) & c(0) \leq p_1, c(q_0-\tau) \geq p_1 \\ (q')^{-1}(q_0 - \tau) & p_0 \leq c(q_0-\tau) < p_1 \\ (q')^{-1})\left(\frac{C/25}{\sum_{t=1}^{25}\frac{1}{(1+\delta)^t}p_0}\right) & c(q-\tau) < p_0, c(q_0) \geq p_0 \\ (q')^{-1}(q_0) & c(q_0) \leq p_0 \end{cases}.$$

The household will optimally install a system large enough to exactly offset all consumption if the levelized cost of electricity generation from the marginal unit capacity is less than or equal to the lowest electricity rate, p_0. It does not install any capacity if the levelized cost of electricity generated from the first unit capacity is greater than the highest grid electricity rate. And if levelized costs of the marginal solar capacity are less than the highest grid electricity rate but higher than the lowest grid electricity rate, then the household optimally sizes the solar array to offset just the fraction of grid electricity consumed at the highest rate, $q_0 - \tau$. Figure 10 depicts these cases for given alternative q's that define c. Solar capacity K is increasing left to right, and grid consumption is increasing right to left.

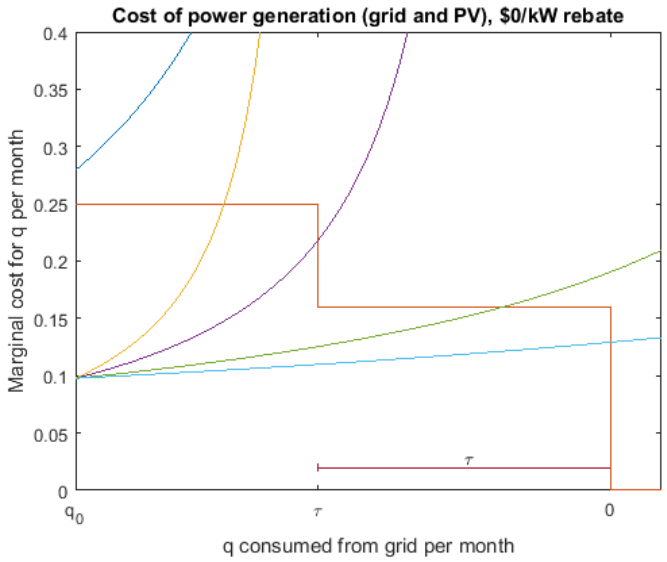


Figure 10: Optimal sizing of solar PV arrays is depicted as a function of alternative modeled q' functions, i.e., the electricity generation of marginal units of solar capacity. Depicted are the costs per kWh for alternative q's and a tariff with two tiers of volumetric charges. Grid consumption increases from right to left. Solar capacity increases left to right.

4.1.1 Sizing Model in PG&E Context

For the purpose of optimal sizing, we convert marginal DC generation to marginal cost per AC kilowatt-hour (kWh) by discounting the flow. This results in the upward-sloping solar price per kilowatt-hour shown in Figure 11, which shows the per-kWh price for three of the home profiles from Figure 5. The optimal installation size, depending on discount rate, is where the discounted marginal cost of solar electricity equals (or becomes higher than) the marginal cost of grid-provided electricity. Figure 12 (top) shows the same houses, but assumes consumption in the 4th bin for the zip code, shifting the dashed lines to the left. Lower consumption results in weakly smaller optimal installation sizes, even when the optimal size does not fully offset consumption. For some homes (e.g. Orange in Figure 12), the optimal installation may be zero panels, which occurs when the marginal cost of electricity generated by even the first panel exceeds the price of the first kWh of offset grid electricity.

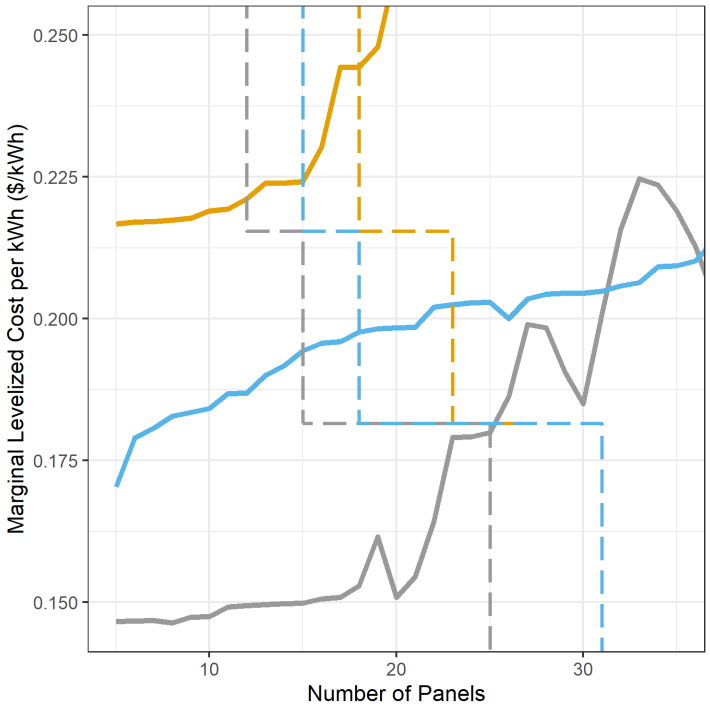


Figure 11: **Irradiance and optimal sizing** Figure shows the marginal per-kWh price of solar generation for a subset of homes from Figure 5 along with the marginal grid price (dashed line) for consumption in the 5th (largest) bin. Marginal grid price varies by climate zone. All homes initially generate solar electricity at a levelized cost below grid electricity. Gray reaches equality between grid and solar marginal cost at 25 panels corresponding to a full offset (Gray will, at optimum, install 25 panels and consume zero electricity from the grid per year). On the other hand, Orange reaches equality at 18 panels, approximately when remaining grid consumption is reduced to the second tier price of $0.215 per kWh. Orange, after an optimal installation, still purchases electricity from the grid, as does Light Blue.

The optimal installation size, K^*, and the corresponding optimal annual generation, q^*, are a function of consumption and irradiance profile of the house. Figure 12 illustrates how consumption and roof profile affect both the payoff of solar – the value of the offset grid electricity over the life of the panel – and the cost of solar. In Figure 11, both Orange and Light Blue are assumed to consume the same amount of electricity. Orange has low irradiance, and installs 18 panels at the optimal, which reduces Orange's grid consumption to τ_2, the level at which these households reach the second pricing tier (around $0.215/kWh). Light Blue also optimally installs 18 panels. However, Light Blue's 18 panels generate more electricity, offsetting grid consumption to the point that Light Blue consumes from the grid τ_1, the level at which these households reach the first pricing tier (around $0.18/kWh). Despite optimally installing the same number of panels at the same cost, Orange offsets less electricity, and Orange's flow benefits are much lower. Gray installs far more panels than Orange and Light Blue, facing a much higher up-front cost, but also offsetting more electricity than Orange or Light Blue. Comparing Gray between Figures 11 and 12 clearly shows the variation owing to different consumption levels: Gray always fully offsets, but does so at 25, 14, and 6 panels for consumption in the 5th, 4th, and 2nd bin, respectively. Variation in the electricity rate structure across climate zones alter the optimal installation

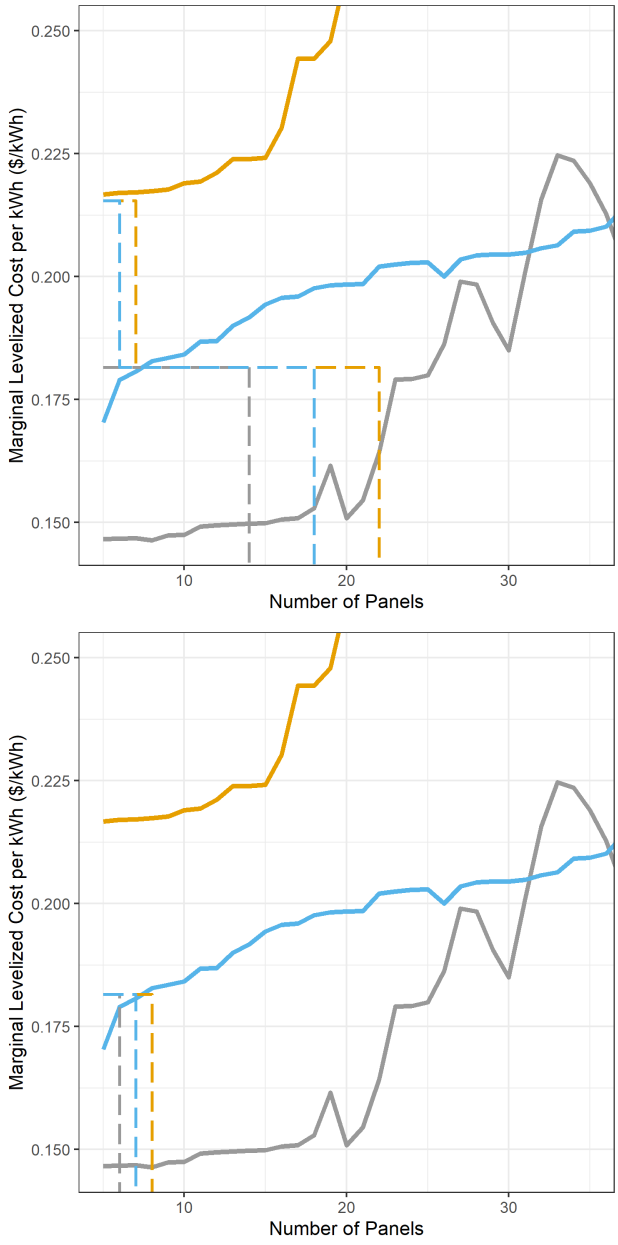


Figure 12: **Irradiance and optimal sizing in the 4th (top) and 2nd bin of consumption (bottom)**. (Top) the optimal installation is weakly decreasing in consumption. With lower consumption, marginal grid prices a lower due to increasing block pricing, the value of offset electricity steps down at smaller numbers of panels, and it reaches a full offset earlier as well. Note that Orange has no amount of generation where the marginal levelized cost per kWh is below the cost of grid electricity. For this consumption level, Orange's optimal installation size is 0. Gray still finds full offset to be optimal, but this occurs at 14 panels. (Bottom) Consumption in the 2nd bin results in small (Blue and Gray) or zero-sized optimal installations (Orange).

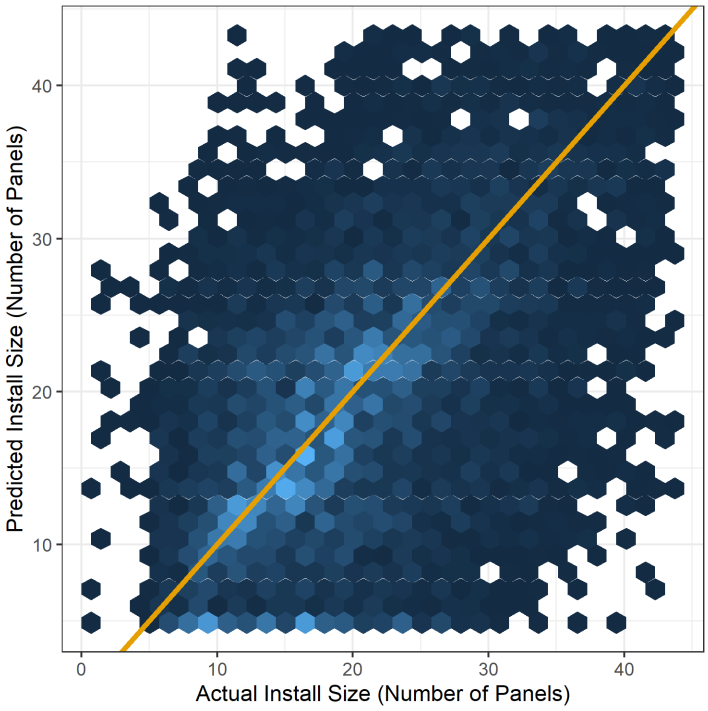


Figure 13: Density plot of Google Sunroof-method predicted (y-axis) and actual (x-axis) installed system capacity. The diagonal represents correct predictions of the optimal installation size.

size (and thus benefit and cost) by compressing or extending the steps in the dashed lines in Figures 5 and 12, as is the case when California eliminated one of the four block pricing tiers. Changes in the rates (step heights) over time occur as well, which moves the steps along the y-axis (not shown).

The optimal sizing model can be compared to the observed installation sizes in the data as we observe the consumption of adopters. Figure 13 shows that the relationship largely holds. This is consistent with installers using similar tools (electricity bills and roof profiles) to size a system.

4.2 Adoption Decision

Once the optimal size has been determined, consumers decide whether or not to install solar. We estimate a dynamic discrete choice model with some similarities to De Groote and Verboven (2016) and Bollinger and Gillingham (2018). We depart from these two papers in exploiting variation in household-level characteristics. We treat the adoption of solar as an exit action in formulating our discrete choice problem. We assume that electricity rates are relatively stable and known, and thus the importance of dynamics enters through changing solar PV prices net of rebates that can result from changing rebates over time. We specify the utility of adopting solar with a random utility expression such that:

$$v_1(q_0, q^*) = u_1(q_0, q^*) = \delta_1 + \sigma\epsilon_1, \tag{1}$$

where δ_1 is utility from adoption of solar, and ϵ_1 is a stochastic term (assumed type 1 extreme value) and σ a scaling parameter, since we normalize the scale through our specification of δ_1.

The utility from the adoption of a solar installation with a lifespan of T, relative to not adopting, is given by:

$$\delta_1 = \int_{q_0 - q^*}^{q_0} \sum_{t=1}^{T} \frac{1}{(1+\rho)^{t-1}} p_t(x)dx - TC(K^*) + X\beta \tag{2}$$

The integrand in 2 reflects the present value of future costs of grid electricity avoided given solar generation of q^*. $TC(K^*)$ is the total cost of the solar installation of optimal size K^*, $X\beta$ is the heterogeneous utility from electricity consumption and ancillary utility derived from solar adoption. It is defined by the per unit price of grid electricity, $p(x)$, which potentially varies (discretely) in x, and by magnitude of grid electricity consumed, which is the difference in total electricity consumption per period, q_0 and the solar power generated by the optimally sized solar PV system q^*.

We omit subscripts for notational convenience and assume the determination of optimal panel size is a static decision in which the household chooses a solar array that minimizes the cost of generating the total quantity of electricity the household consumes, which depends upon electricity consumption and price, as well as rooftop irradiance.

Let us assume that electricity prices evolve according to $p'(x) = (1+\zeta)p(x)$ and panels depreciate each year by λ, such that $q' = (1-\lambda)q$. The expression for the economic value of adoption over the life of the solar array can be simplified to:

$$\delta_1 = \theta q^* \bar{p} - TC(K^*) + X\beta, \tag{3}$$

in which we define:

$$\theta = \sum_{t=1}^{T} \left((1+\zeta)(1-\lambda)\rho\right)^{(t-1)} \tag{4}$$

$\theta q^* \bar{p}$ captures the utility of electricity consumption over the installation's life and $\bar{p}$ is the current average cost of grid electricity avoided by adoption.[7] We also need to make some assumption of what consumers expect to do after the lifetime of their solar array. We treat the dynamic problem as a fixed-time problem, as in De Groote and Verboven (2016). The value for installing solar is given by $V_1 = \delta_1 + \sigma\epsilon_1$.

When not adopting solar, the consumer pays the full cost of grid electricity in the current period (reflected in the avoided cost expression for δ_1) but gains the continuation value in the next period. Upon examination, the decline in solar PV costs appear to be in the variable costs such that $TC(K^*) = FC + VC(K^*)$ in which $VC(K^*)' = \eta VC(K^*)$. We assume type I extreme value shocks for ϵ_0 and ϵ_1. We can write an expression for the value of non-adoption using conditional choice probabilities (Hotz and Miller 1993), treating adoption as an exit state, as in De Groote and Verboven (2016) and Bollinger and Gillingham (2018):

$$\begin{aligned} \delta_0 &= \rho\left(\int V_1' - \ln(Pr_1')dF(TC'|TC) + \gamma\right) \\ &= \rho(1+\zeta)\theta q^*\bar{p} - \rho FC - \rho\eta VC(K^*) + \rho X\beta - \sigma\rho\ln(Pr') + \sigma\rho\gamma \end{aligned} \tag{5}$$

in which γ is Euler's constant, V_1' is the next period adoption utility, and Pr_1' is the adoption probability next period, both of which are a function of the expected cost of the installation (net of any rebates) in the next period, TC'.

Thus, the value of non-adoption, $V_0 = \delta_0 + \epsilon_0$, is simply a function of the expected value of adopting, given by V_1, in both the current period and next period, as well as the probability of adopting in the next period.

We can calculate the difference in our expressions for δ_1 and δ_0 in equations (3) and (5) which yields the difference in the value of adopting versus not adopting:

$$\begin{aligned} \delta_1 - \delta_0 &= (1-\rho(1+\zeta))\theta q^*\bar{p} - (1-\rho)FC - (1-\rho\eta)VC \\ &+ (1-\rho)X\beta + \sigma\rho\left(\log(Pr') - \gamma\right) \end{aligned} \tag{6}$$

We can estimate the transition of the installation costs η, the transition of electricity prices ζ, and the probability of adoption in a first stage.

[7] As solar output declines gradually, it is possible for $\bar{p}$ to also change slightly with tiered pricing, but we will account for this in the estimation of how average price changes for different consumption bins over time.

For lease systems, the economic value of the lease over its lifespan is:

$$\delta_1^l = \theta q^* \bar{p} - \theta^{ppa} q^* p^{ppa} + X\beta, \tag{7}$$

in which we define:

$$\theta^{ppa} = \sum_{t=1}^{T} ((1+\zeta^{ppa})(1-\lambda)\rho)^{(t-1)} \tag{8}$$

in which p^{ppa} is the starting price of solar electricity and ζ^{ppa} captures the annual change in the electricity price guaranteed by the PPA, which we set at .04 based on industry standards.

Now, the price the installer should charge for the solar electricity should reflect the levelized cost of installing the system:

$$p^{ppa} = \frac{TC(K^*)}{\theta^I q^*} + transfer \tag{9}$$

in which the θ^I reflects the discounted sum of benefits per kWh using the installer's discount rate:

$$\theta^I = \sum_{t=1}^{T} \left((1+\zeta^{ppa})(1-\lambda)\rho^I\right)^{(t-1)} \tag{10}$$

plus some extra transfer to the installer for fronting the installation costs. We might assume this transfer to be the same for all leases, but it is also likely it would be the same per dollar spent on the installation, i.e. it would scale by the system cost. It is also possible it may take the form of a per-kWh markup. Let us write 9 as:

$$p^{ppa} = TC(K^*)(1+\kappa^{TC})\frac{1}{\theta^I}\frac{1}{q^*} + \kappa^p \tag{11}$$

κ^{TC} captures the profit margin based on the per dollar cost of providing the capital for the installation, and κ^p captures a per-kWh markup. The first multiplicative factor in 11 applies the markup to $TC(K^*)$, then divides by θ^I, which amortizes the marked-up cost over 25 years at the installers discount rate (just as θ converts a flow of benefits to a present value). Finally, the amortized cost is divided by the per-period generation q^*, plus a per-kWh markup.

By substitution, for lease systems, the economic value of the lease over its lifespan can thus be written:

$$\delta_1^l = \theta q^* \bar{p} - \theta^{ppa} q^* \kappa^p - \frac{\theta^{ppa}}{\theta^I}(1+\kappa^{TC})TC(K^*) + X\beta, \tag{12}$$

The difference in the expression for δ_1^l and δ_0^l for consumers who would lease is:

$$\begin{aligned} \delta_1^l - \delta_0^l &= (1-\rho(1+\zeta))\left(\theta q^* \bar{p} - \theta^{ppa} q^* \kappa^p\right) \\ &- \frac{\theta^{ppa}}{\theta^I}(1+\kappa^{TC})\Big((1-\rho)FC + (1-\rho\eta)VC\Big) \\ &+ (1-\rho)X\beta + \sigma\rho(\log(Pr^{l'}) - \gamma) + \sigma\epsilon \end{aligned} \tag{13}$$

Note that this expression is very similar to that for purchases, since the costs of the panels are reflected in the PPA price. The only difference is the $\frac{\theta^{ppa}}{\theta^I}(1+\kappa)$ multiplier in front of the terms that capture the cost of the solar panels. Leasing has the effect of amortizing the cost of installing over the life of the panels. The term before the panel cost in 6 is less than 1 for households whose discount rates are sufficiently higher than the installer's discount rates to overcome the markup κ^{TC}. We assume a rate of return on investment (κ^{TC}) markup captures the full resolution of p^{PPA} and assume κ^P, a per-kWh markup in 14, is equal to zero.

The probability of adoption conditional on consumption bin and being in the purchase market is:

$$Pr^p = \Lambda\left(\frac{1}{\sigma}\left(\bar{V}_1 - \bar{V}_0\right)\right) \tag{14}$$

in which $\bar{V}_1$ and $\bar{V}_0$ are the deterministic portions of the value of adopting shown in equation 6 and Λ is the standard Logit cdf. Similarly,

$$Pr^l = \Lambda\left(\frac{1}{\sigma}\left(\bar{V}_1^l - \bar{V}_0^l\right)\right) \tag{15}$$

is the probability of leasing, conditional on being in the lease market.

5 Estimation

5.1 Unobserved heterogeneity

Estimation of the household-level adoption model can be done via maximum likelihood estimation. In the infeasible case where purchase/lease type $e \in \{\text{lease, purchase}\}$ and consumption bin $b \in \{1, ..., 5\}$ is observed, each household's contribution to the likelihood is written as:

$$\mathbb{L}_{ibe} = \prod_t [Pr_{ibt}^e]^{y_{it}} [1 - Pr_{ibt}^e]^{(1-y_{it})} \tag{16}$$

where Pr_{ibt}^e is the probability of household i adopting in time t, conditional on being type e and bin b.

In practice, we do not observe the consumption bin b, nor the type e for non-adopting households. We use the method of Arcidiacono and Miller (2011), treating the combination of consumption bin b and type e as permanent, unobserved heterogeneity. Each non-adopter household is one of ten possible consumption $\times$ type combinations $\{1, ..., 5\} \times \{\text{leaser, purchaser}\}$. We specify weights w_{ibe} as the probability that household i consumes in consumption bin b and is of type e. With weights w_{ibe}, we integrate the likelihood function over the unobserved heterogeneity:

$$\mathbb{L} = \prod_i \sum_b \sum_e w_{ibe} \prod_t [Pr^e_{ibt}]^{y_{it}} [1 - Pr^e_{ibt}]^{(1-y_{it})} \tag{17}$$

which requires evaluating ten conditional likelihoods per observation of household i and time t.

We posit the weights w_{ibe} as $w_{ib} \times w_{ie}$, where the following adding up constraints apply:

$$\begin{aligned} &\textstyle\sum_{e'=1}^{2} w_{ie'} = 1 \\ &\textstyle\sum_{b'=1}^{5} w_{ib'} = 1 \\ &\textstyle\sum_{i \in z} w_{ib} = \frac{N_z}{5} \end{aligned} \tag{18}$$

The first two constraints require that each household i have weights that sum across consumption bin b and type e to equal 1. The constraint in 18 requires that, within a zipcode z, the weights must sum to 1/5th of the number of households in the sample for that zipcode (due to the use of quntiles). This guarantees that the moments of the consumption distribution match the empirical distribution.

The constraint in 18 makes w_{ibe} dependent on w_{jbe} for any $i \in z, j \in z$. Methods of calculating these weights such as those in Arcidiacono and Miller (2011) are not appropriate for dependent weights, and an alternative is employed here. To account for dependence, we integrate over randomly drawn allocations of b that comport with the empirical distribution.

1. Draw $R = 1000$ random allocations of b that place $\frac{1}{5}$ of the households into a randomly selected bin, guaranteeing that $b^{(r)}$, the r^{th} allocation, satisfies the constraint in 18 for each allocation r
2. Evaluate the conditional likelihood for every $\{b, e\}$ combination for every household i and time t, then taking the likelihood as the product over t, calling this $L_{ibe} = \Pi_t L_{ibet}$
3. Calculate $w_{ie|b}$, the type-weight, for each L_{ibe} as $\frac{L_{ie|b}}{L_{ie|b} + L_{ie'|b}}$, following Arcidiacono and Miller (2011)
4. Calculate L_{ib} as the $w_{ie|b}$-weighted sum of L_{ibe}
5. Turning to the b weights, for each r, calculate the likelihood of observing r conditional on the parameters and $w_{ie|b}$. To do so, take the product of $L_{ib^{(r)}}$ where $L_{ib^{(r)}}$ is the likelihood for household i conditional on being in the bin drawn in allocation r. Formally, $L_r = \Pi_i L_{ib^{(r)}}$
6. Calculate allocation weights $w_z^{(r)} = \frac{L_r}{\sum_r L_r}$
7. Calculate $L_z = \sum_r w_z^{(r)} L_r$

8. Log-likelihod $L = \sum_z log(L_z)$

Allocations r where households are better allocated to consumption bins b that better explain the observed outcome are weighted higher than allocations that poorly explain the observed outcome. All weights sum to 1 within household i, and all weights satisfy 18 by definition.

5.2 Conditional Choice Probabilities

The final component of 17 is the conditional choice probability (CCP), which is the predicted probabilities of adopting in the next period. We again follow Arcidiacono and Miller (2011) and use a flexible logit[8] to estimate the probability of adopting for household h at time t. Weights w_{ibt} are used in the flexible logit and a separate probability of adopting is estimated for leasers and purchasers. In estimation, the next-period probability of adopting $Pr_{ib}^{e'}$ is updated in a third step, following the update of the weights. The flexible logit is specified using all interactions of the variables in X, along with time fixed effects and boundary zone fixed effects, as are used in the structural model. The CCP's (predicted probabilities of adopting in the next period) are generated by advancing the time by 1 period and predicting the logit response.

5.3 Estimation transformations

For estimation, σ is estimated as e^{σ} to preserve positive variance. The parameters of ρ are estimated with a Normal cdf transformation $\rho_i = \Phi\left(\rho + \alpha_{low} 1(\text{wealth}_i{=}\text{low}) + \alpha_{med} 1(\text{wealth}_i{=}\text{med})\right)$

6 Results

6.1 Structural Parameters

[8] A bin estimator would be feasible, but components of 6 and 14 are continuous

Table 2: Structural parameter results

Param. Grp	Parameter	Estimate	se	t	pval
σ	σ	1.790	0.004	449.408	0.000***
ρ	ρ_{high}	1.966	0.097	20.248	0.000***
	α_{med}	0.008	0.278	0.029	0.977
	α_{low}	-0.262	0.100	-2.615	0.009**
β	Wealth: lowest 1/3rd	-107.118	3.000	-35.706	0.000***
	Wealth: middle 1/3rd	-8.092	1.333	-6.072	0.000***
	β_0	87.276	1.199	72.771	0.000***
	Voter Affiliation: D	0.868	2.340	0.371	0.711
	Length of residence	-0.104	2.321	-0.045	0.964
	Child	6.851	2.560	2.676	0.007**
	Stories	-34.287	1.829	-18.750	0.000***
	Sqft (1,000's)	39.516	9.245	4.274	0.000***
	Sqft^2	-2.727	40.572	-0.067	0.947
	Lease x Wealth: β_0	-102.320	17.887	-5.720	0.000***
	Lease x Wealth: lowest 1/3rd	77.075	6.701	11.502	0.000***
	Lease x Wealth: middle 1/3rd	33.852	15.704	2.156	0.031*
γ_{area}	γ_B	8.319	16.615	0.501	0.616
	γ_C	10.156	3.622	2.804	0.005**
	γ_D	-6.763	31.036	-0.218	0.827
$\phi_{consumption}$	ϕ_{bin1}	-4.399	2.573	-1.710	0.087.
	ϕ_{bin2}	-29.351	38.037	-0.772	0.440
	ϕ_{bin3}	-14.147	13.781	-1.027	0.304
	ϕ_{bin4}	-11.918	8.922	-1.336	0.181
$\tau_{time \times wealth}$	τ_{2014Q2}	39.972	8.818	4.533	0.000***
	τ_{2014Q3}	36.251	8.455	4.287	0.000***
	τ_{2014Q4}	-8.211	59.269	-0.139	0.889
	τ_{2015Q1}	3.192	15.194	0.210	0.834
	τ_{2015Q2}	-1.014	54.767	-0.019	0.985
	τ_{2015Q3}	-30.266	14.920	-2.029	0.042*
	τ_{2015Q4}	75.264	3.456	21.775	0.000***
	τ_{2016Q1}	51.257	6.557	7.817	0.000***
	τ_{2016Q2}	7.780	5.793	1.343	0.179
	$\tau_{2014Q2L}$	-11.792	7.247	-1.627	0.104
	$\tau_{2014Q3L}$	-14.773	5.009	-2.949	0.003**
	$\tau_{2014Q4L}$	40.047	30.811	1.300	0.194
	$\tau_{2015Q1L}$	-2.167	7.425	-0.292	0.770
	$\tau_{2015Q2L}$	30.766	15.727	1.956	0.050.
	$\tau_{2015Q3L}$	82.189	9.573	8.586	0.000***
	$\tau_{2015Q4L}$	-23.950	17.712	-1.352	0.176
	$\tau_{2016Q1L}$	-7.066	11.193	-0.631	0.528
	$\tau_{2016Q2L}$	-26.609	1.693	-15.715	0.000***
	$\tau_{2014Q2M}$	-14.933	3.486	-4.284	0.000***
	$\tau_{2014Q3M}$	-4.499	2.128	-2.114	0.034*
	$\tau_{2014Q4M}$	13.516	13.831	0.977	0.329
	$\tau_{2015Q1M}$	11.021	2.559	4.306	0.000***
	$\tau_{2015Q2M}$	16.979	10.642	1.596	0.110
	$\tau_{2015Q3M}$	71.472	9.655	7.403	0.000***
	$\tau_{2015Q4M}$	-29.040	6.212	-4.675	0.000***
	$\tau_{2016Q1M}$	-37.036	7.463	-4.963	0.000***
	$\tau_{2016Q2M}$	-30.672	6.534	-4.694	0.000***

[1] Robust std. errors from Arcidiacono and Miller (2011)

The estimated parameters are as expected. We find negative effects for low and medium wealth in the intercept, relative to high wealth (omitted), while intercept shifts for leasers show large negative values for high-wealth (Lease x Wealth: β_0) and positive shifts for leasing for medium and low wealth households. The parameter on square footage is increasing with a negative quadratic term. The positive sign for voter affiliation indicates Democratic or Green party registered households derive more utility from adopting solar, though the difference is not statistically distinguishable from zero. Square footage is positive in the linear term and close to zero in the quadratic, while 2+ stories is negative indicating single-story homes receive more utility from adopting relative to equal-sized two-story homes, possibly due to greater roof area for optimal solar panel siting. Fixed effects for consumption bins show a U-shaped form: the lowest consumption bin, ϕ_{bin1} is closest to the omitted category, bin 5, while ϕ_{bin2} is the lowest. This is consistent with households that are highly energy-cognizant investing in energy efficiency *and* solar adoption.

The parameters of interest are ρ, the discount rate for high-wealth households, as well as α_{low} and α_{med}, the shifts for low- and medium-wealth households. Before transforming to an annual discount rate[9], the sign and significance indicates that medium wealth households have a lower discount rate, though the difference is statistically insignificant. α_{low} indicates a higher discount rate for low-wealth households, and is statistically significant.

6.2 Discount Rates

Transforming the results in Table 2 results in annual implicit discount rates of:

$$\delta_{high} = 10.5\%$$
$$\delta_{med} = 10.3\%$$
$$\delta_{low} = 19.8\%$$

Parameter estimates can be used to calculate θ_i using Equation 4. θ_i converts a \$1 annual flow of electricity costs avoided by installing solar into a present value, taking into account panel decline and expected electricity price increases. The ratio of θ for low-wealth households to high- or medium-wealth households quantifies the value of the flow subsidy between low- and high-/med-wealth households.

Since θ_i is a function of grid electricity rate increases (ζ) and a common depreciation rate (λ), we take the weighted average of θ_i over each of the wealth bins. Weights are the probability of being in each consumption bin and type[10] w_{ibe}. We take the weighted average θ for high-wealth households, which is 50.6. The weighted mean θ for low-wealth households is 27.6, a factor of 1.8. Therefore, we find that high-wealth households, on average, value a flow of net metering benefits 1.8 times higher than low-wealth households value the exact same flow.

We calculate an equivalent $\theta_{4\%}$, which converts the flow of net metering benefits to present value using a discount rate of 4%. This reflects the approximate cost of borrowing for a government entity. At 4%, the value of $\theta_{4\%}$ is 95.22. The average θ across all wealth bins is \$42.64. That is, the present value

[9] $\Phi(\rho_i)^{-4} - 1$ as the time step is quarterly

[10] θ_i does not vary with type, but ζ does vary by consumption bin and zip code

to a government entity of providing a flow of benefits equivalent to net metering is about $\frac{95.22}{42.64} = 2.23$ times the valuation of the average household. At an average $q^*\bar{p}$ per year of \$870 (or \$217.38 per quarter period), the present value of the flow to average household is \$9,268, while the same figure for a government entity using $\theta_{4\%}$, the value is \$20,703. For scale, the average after-tax-credit cost of a system is \$9,268. The value of the benefits to the government exceeds the present value of the benefits to the household by \$11,434 for the average installation. Alternatively, one could propose a net metering policy where the flow benefits are cut in half, reducing the present value of the flow to the average household by \$4,297.50, but up-front incentives are increased by that amount, reducing the installation cost by around 1/3. An average household would be indifferent to adoption before and after this change.

Table 3: Average discount rates and implied valuation for flow benefits

Avg. Discount Rate	θ	$\theta_{4\%}$	ratio
13.67%	42.64	95.22	2.23

[a] $\theta_{4\%}$ is value to government entity discounting at 4%

Table 4: Valuation of average flow relative to up-front total cost, full sample and adopters-only

Adopter	Average TC	Average $q^*\bar{p}$	$\bar{\theta}$	$\bar{\theta}q^*\bar{p}$	$\bar{\theta}_{4\%}q^*\bar{p}$
All	\$9,957.93	\$217.38	42.64	\$9,268.21	\$20,702.55
Adopters Only	\$13,658.51	\$329.55	42.71	\$14,074.74	\$29,831.90

Table 5: Valuation of flow benefits by wealth bins

Wealth	Annual Discount Rate	$\bar{\theta}$	ratio
High	10.5%	50.6	1.8
Med	10.3%	51.6	1.9
Low	19.8%	27.6	1.0

7 Counterfactual Analyses

7.1 Counterfactual Methodology

Under counterfactual regimes, we must account for the fact that the probability of adopting in the next period will also change. I.e., counterfactuals require counterfactual CCP's – as the utility payoff of adopting changes (in one or all periods), the probability of adopting in the next period also changes. Here, we attempt to use model estimates to update both $\delta_1 - \delta_0$ and $log(Pr')$ as well.

Our strategy for calculating $log(Pr^{'+})$ is to calculate the *difference* in adoption utility implied by the estimated parameters of the model. Arcidiacono and Miller (2020) discuss identification of counterfactual CCPs and show conditions under which counterfactual CCPs are identified. Under strong assumptions of stationarity, counterfactual CCPs are identified as the "choice probabilities from the past fully capture anything that might happen in the future". We assert that the progression of electricity prices and solar costs form a stationary environment, allowing us to identify both model parameters and CCPs in our setting.

We rely on the flexible logit estimate of $log(Pr^{'})$ and the model-implied *differences* in flow payoff to calculate future values of counterfactuals $log(Pr^{'+})$. Our strategy is to leverage the stationarity of the environment to re-write future changes in the probability of adopting as an infinite series of (known) flow utility payoffs.

Let A capture the scaled (by $1/\sigma$) utility of adopting today relative to the discounted utility of adopting tomorrow, $A = (u - \rho u')/\sigma$, and B capture the next period adoption probability and Euler constant, so that we can write the value of adopting as:

$$\begin{aligned}\frac{1}{\sigma}(\delta_1 - \delta_0) &= \overbrace{\frac{1}{\sigma}(1-\rho(1+\zeta))\theta q^* \bar{p} - \frac{1}{\sigma}(1-\rho)FC - \frac{1}{\sigma}(1-\rho\eta)VC + \frac{1}{\sigma}(1-\rho)X\beta}^{A} \\ &+ \underbrace{\rho\left(\log(Pr') - \gamma\right)}_{B}\end{aligned}$$

Under a counterfactual scenario, we change the utility of adopting today by Δu and the expected utility of adopting tomorrow by $\Delta u'$, so that $\Delta A = (\Delta u - \rho \Delta u')/\sigma$.

The counterfactual change in the probability of adopting, Pr^+, is determined by the change in A plus the change in B:

$$Pr^+ = \Lambda\left(\frac{1}{\sigma}(\delta_1 - \delta_0) + \Delta A + \Delta B\right)$$

Note we can write:

$$\Lambda^{-1}(Pr) = log\left(\frac{Pr}{1-Pr}\right)$$

and thus

$$\begin{aligned}log(Pr') &= \Lambda^{-1}(Pr') + log(1-Pr') \\ &= \frac{1}{\sigma}\left(\delta_1^{'} - \delta_0^{'}\right) + log(1-Pr'), \end{aligned} \tag{19}$$

where $\delta_1^{'}$ is the next-period utility of adopting and $\delta_0^{'}$ is the next period utility of non-adoption. Using this expression, we can write B as:

$$\begin{aligned}B &= \rho(log(Pr^{'}) - \gamma) \\ &= \rho\left(\frac{1}{\sigma}(\delta_1^{'} - \delta_0^{'}) + log(1-Pr')\right) - \rho\gamma\end{aligned}$$

and we can write B^+ (the value of B under the counterfactual) as:

$$\begin{aligned}B^+ &= \rho\left(log(Pr^{'+}) - \gamma\right) \\ &= \rho\left(\frac{1}{\sigma}(\delta_1^{'+} - \delta_0^{'+}) + log(1-Pr^{'+})\right) - \rho\gamma\end{aligned}$$

Thus, the change in B is equal to:

By plugging in the values for δ and δ^{+} (see Appendix XX), we can write the change in B as:

$$\Delta B = B^{+} - B = \Delta A^{'} + \rho \Delta B^{'} + \rho(log(1 - Pr^{'+}) - log(1 - Pr^{'})), \tag{20}$$

where $\Delta B^{'}$ is the next-period discounted difference between counterfactual and actual $log(Pr^{'})$. We denote the next period's next-period logged probability of adopting as $log(Pr^{''})$ and $log(Pr^{''+})$, and additional future probabilities of adopting as $log(Pr^{'}_{s}$ and $log(Pr^{'}_{s}{}^{+}$ where s is the number of periods into the future. ΔB is a recursive sum. Each recursion produces $\Delta A'$ that is equal to ΔA scaled by ρ

and η, as well as a discounted difference in logged probability of *not* adopting s periods ahead (details in Appendix XX):

$$\Delta B = \sum_{t=1}^{\infty} \rho^t \Delta A_t + \sum_{s=1}^{\infty} \rho^s \left(log \left(\frac{1 - Pr_s^{'+}}{1 - Pr_s^{'}} \right) \right) \tag{21}$$

where the t subscript on A_t indicates the fact that A can change in future periods based on the evolution of the state variables that are affected by the counterfactual changes (electricity prices, solar prices, etc.). Adoption probabilities are very small and thus we approximate:

$$log \left(\frac{1 - Pr_s^{'+}}{1 - Pr_s^{'}} \right) \approx 0. \tag{22}$$

This means we can write:

$$\Delta A + \Delta B = \sum_{t=0}^{\infty} \rho^t \Delta A_t = \sum_{t=0}^{\infty} (\Delta u_t - \rho \Delta u_{t+1}) = \frac{1}{\sigma} \Delta u_t. \tag{23}$$

For example, if we change the variable costs such that VC is scaled by $\frac{1}{c}$ in all periods, this reduces variable costs by $(c-1)/c$ and the current-period t change in the utility of adopting is:

$$\Delta A + \Delta B = \frac{1}{\sigma} \left(\frac{c-1}{c} VC \right) \tag{24}$$

Now let us write the next period differences in the counterfactual value of adopting relative to not adopting as:

$$\frac{1}{\sigma} \left(\delta_1^{'+} - \delta_0^{'+} \right) = \frac{1}{\sigma} \left(\delta_1^{'} - \delta_0^{'} \right) + \overbrace{\Delta A \eta}^{\Delta A'} + \overbrace{\rho(log(Pr^{''+}) - log(Pr^{''}))}^{\Delta B'}$$

Recall

$$Pr' = \frac{1}{1 + \exp(-(\delta_1' - \delta_0')/\sigma)} \tag{25}$$

and so by rearranging terms, we have:

$$1/Pr^{'+} - 1 = \exp(-(\delta_1^{'} - \delta_0^{'})/\sigma)) \exp(-\Delta A' - \Delta B') \tag{26}$$

$$= (1/Pr^{'} - 1) \exp(\Delta A' + \Delta B') \tag{27}$$

So this gives us the change in $Pr^{'}$ under the counterfactual:

$$Pr^{'+} - Pr^{'} = Pr^{'} \left(\frac{1}{(1 - Pr^{'}) \exp(-\Delta A' - \Delta B') + Pr'} - 1 \right) \tag{28}$$

7.2 Counterfactual Results

We explore the outcomes of two counterfactual policies. First, a 1% reduction in the variable cost (per Watt capacity), allowing us to calculate a demand elasticity. Second, we approximate the proposed "Net Metering 3.0" updates to California's Net Metering policy as discussed in Section 2. We operationalize this scenario using the estimated avoided cost payout for a typical solar generation profile established in the CPUC Avoided Cost Calculator report from E3 consulting (E3, 2022), which estimates a levelized cost of energy (LCOE) of \$.062/kWh. This figure represents the levelized value of solar generation according to a typical solar generation and consumption profile.

All counterfactual scenarios report the total number of predicted adoptions occuring within the study sample and during the study period. In all cases, we calculate adoption as one minus the joint probability of choosing "do not adopt" in each of the 10 time periods in the study window. This allows us to report the total number of adoptions predicted over the period, rather than examining across time periods. We construct counterfactuals such that the counterfactual price and NEM policy changes are expected to remain in place for the future. The methods presented in the previous section allow us to adjust future adoption probabilities to reflect the counterfactual, leveraging the assumption of stationarity following the end of the study period.

7.2.1 1% Reduction in Panel Cost

This counterfactual scenario reports the total predicted adoptions under a 1% reduction in the panel cost. The purpose is straightforward – to calculate the model-predicted elasticity of demand. Table 6 shows the ratio of counterfactual to baseline adoptions under scenario 1, a 1% reduction in panel costs.

Under this scenario, high-wealth households increase adoption by 2.4%, while medium-wealth households increase adoption by 2.0% and low-wealth households increase adoption by only 0.9%. The average response of 1.8% is in line with previous reduced form estimates of demand elasticity.

Table 6: Scenario 1: 1% decrease in up-front variable cost; ratio of counterfactual to baseline adoption

		1% Decrease in Up-Front Variable Cost		
Wealth	Rate	Counterfactual Installations	Counterfactual Purchases	Counterfactual Leases
HIGH	10.5%	1.024	1.026	1.020
MED	10.3%	1.020	1.023	1.016
LOW	19.8%	1.009	1.014	1.006
All	–	1.018	1.022	1.013

Table 7: Scenario 1: 1% decrease in up-front variable cost; predicted adoptions

		1% Decrease in Up-Front Variable Cost				
Wealth	Rate	Households	Observed Adopt	Share Obs. Adopt	Counterfactual Adopt	Share Counterfactual Adopt
HIGH	10.5%	50298	2009	3.99%	2058	4.09%
MED	10.3%	67631	3272	4.84%	3336	4.93%
LOW	19.8%	65738	1963	2.99%	1981	3.01%
All	–	183667	7244	3.94%	7375	4.02%

7.2.2 $.062 per kWh NEM

In Section 7.2, we discuss the proposed Net Metering 3.0 revisions approved by the CPUC in December 2022. Our second counterfactual examines the outcome under a revision only to the NEM rate as determined by the 2022 Avoided Cost Calculator (E3, 2022), which serves as the underlying input for the value of rooftop solar generation for the revisions. The levelized cost is calculated as the quantity-weighted average value of rooftop solar net generation. Much of this value comes from reducing total consumption from the grid, while some of this value comes from net exports of rooftop solar generation, which occurs when generation exceeds consumption at some instant. A levelized $.062/kWh accounts for the value of offset consumption when consumption exceeds generation, and times in which generation exceeds consumption under a typical load profile and the household is paid the grid avoided cost. For more information on the proposed NEM policy and the $.062/kWh, see Appendix A of the proposed decision.

Table 8 shows the ratio of counterfactual to baseline adoptions in the study period and sample. High- and medium-wealth households with discount rates of 10.5% and 10.3%, respectively, show the largest drop in counterfactual adoptions by 78% and 75%. Low-wealth households, who are less attuned to the flow of benefits, drop by only 43% overall, though from a lower baseline (see Table 9).

Table 8: Scenario 2: Reformed NEM rate; percent counterfactual adoptions relative to baseline

		NEM Proposed $.062/kWh Rate		
Wealth	Rate	Counterfactual Installations	Counterfactual Purchases	Counterfactual Leases
HIGH	10.5%	22.1%	22.6%	20.8%
MED	10.3%	25.1%	24.9%	25.3%
LOW	19.8%	57.0%	56.9%	57.2%
All	–	32.7%	30.6%	35.2%

[a] Avg. offset price in sample: $0.17/kWh. Avg. offset price for adopters: $0.20/kWh.

Table 9: Scenario 2: Reformed NEM rate; predicted adoptions

		NEM Proposed $.062/kWh Rate				
Wealth	Rate	Households	Observed Adopt	Share Obs. Adopt	Counterfactual Adopt	Share Counterfactual Adopt
HIGH	10.5%	50298	2009	3.99%	443	0.88%
MED	10.3%	67631	3272	4.84%	822	1.22%
LOW	19.8%	65738	1963	2.99%	1120	1.70%
All	–	183667	7244	3.94%	2371	1.29%

8 Conclusion

This paper provides a compelling method and setting for identifying heterogeneous household discount rates. These rates are relevant both generally, and to the context of residential adoption of renewable generation. The nature of many "green" technologies is that a large up-front investment pays off over long periods of time. When the "green" technology has positive spillovers to air quality or carbon emissions, policymakers who wish to capture these spillover benefits must consider the individual or household adoption decision. The household discount rate identified here is a key part of this decision when flows payoffs last for greater than 20-25 years.

We leverage novel and plausibly exogenous variation in solar payoffs to identify the key parameters – the household discount rate – applied by households in California in the solar adoption decision. We show model-free evidence that high- and medium-wealth households are more responsive to the value of the solar flow payoff obtained by investing in solar panels. We then estimate a structural dynamic model that pins down heterogeneity in discount rates by wealth. Our results help explain the noted disparities in solar adoption rates between low- and high-wealth households.

Substantive contributions to the literature are made in methods of estimating the model with allowances for unobserved heterogeneity in prior consumption. We also contribute to the literature on counterfactual identification in Conditional Choice Probability models. In the consumption dimension of unobserved heterogeneity, we introduce a method for applying the Expectation Maximization (EM) algorithm to contexts where there is joint dependence in the unobserved heterogeneity in the sample – in our context, accounting for the fact that each of the five consumption bins must have an equal number of households in it. Finally, we leverage the stationarity assumption to note that counterfactuals can be generated as differences in the utility of adopting in the next period, and show that the recursive sum of differences in future adoption can be expressed in a closed form.

The policy applications of our results are clear and timely. As California (and many other states) reform net metering policies to better reflect the actual value of solar generation, and to address equity issues with legacy utility costs, it is important for policymakers to understand how consumer responses to net metering reform may vary by household wealth. We first show that demand elasticity is approximately 2%, with low-wealth households exhibiting 0.9% and high-wealth households exhibiting 2.4%. We show that a significant reduction in the flow payoff of net metering as would be inherent in an "avoided cost" net metering scheme will reduce solar adoption by 67%, but with a larger reduction for high- and medium-wealth households (78 and 75%, respectively). Combined with an "up-front" subsidy, the effect is two-fold: first, the reduction in flow payoffs closes the gap between household wealth groups and adoption rates, largely by reducing high-wealth households' likelihood of adoption. As we show, it is likely that there exists a "sweet spot" where a combination of flow payoff reductions and up-front subsidies can obtain a fixed level of adoption at *lower* cost to utilities and taxpayers, and with benefits spread equitably across wealth levels rather than concentrated among high- and medium-wealth households.

References

Aldy, Joseph E., Todd D. Gerarden, and Richard L. Sweeney, "Capital versus Output Subsidies: Implications for Alternative Incentives for Wind Investment," 2017, (Working Paper).

Allcott, Hunt and Nathan Wozny, "Gasoline prices, fuel economy, and the energy paradox," *Review of Economics and Statistics*, 2014, *96* (5), 779–795.

Arcidiacono, Peter and Robert A Miller, "Conditional choice probability estimation of dynamic discrete choice models with unobserved heterogeneity," *Econometrica*, 2011, *79* (6), 1823–1867.

_ **and Robert A. Miller**, "Identifying Dynamic Discrete Choice Models off Short Panels," *Journal of Econometrics*, April 2020, *215* (2), 473–485.

Barbose, Galen, Naim Darghouth, Samantha Weaver, and Ryan Wiser, "Tracking the Sun VI: An Historical Summary of the Installed Price of Photovoltaics in the United States from 1998-2012," Technical Report, Lawrence Berkeley National Laboratory, Berkeley, CA July 2013.

Bento, Antonio M, Shanjun Li, and Kevin Roth, "Is there an energy paradox in fuel economy? A note on the role of consumer heterogeneity and sorting bias," *Economics Letters*, 2012, *115* (1), 44–48.

Bollinger, Bryan and Ken Gillingham, "Social Learning and Solar Photovoltaic Adoption: Evidence From a Field Experiment," 2018, (Working Paper).

Borenstein, Severin and Lucas W Davis, "The distributional effects of US clean energy tax credits," *Tax Policy and the Economy*, 2016, *30* (1), 191–234.

De Groote, Olivier and Frank Verboven, "Subsidies and Myopia in Technology Adoption: Evidence from Solar Photovoltaic Systems," 2016, (Working Paper).

Dubin, Jeffrey A and Daniel L McFadden, "An econometric analysis of residential electric appliance holdings and consumption," *Econometrica*, 1984, pp. 345–362.
E3 Consulting (E3)

E3 Consulting (E3), "Avoided Cost Calculator v1a," Technical Report, E3 Consulting, San Francisco, CA 2022. Online at `https://e3.sharefile.com/share/view/s3fdd4ff8b9db4e95904726427ae54e81/fo5e3775-f03c-4008-be45-9e8d3e765955`. Last visited 2022-07-01.

Gillingham, Kenneth and Tsvetan Tsvetanov, "Hurdles and steps: Estimating demand for solar photovoltaics," Technical Report, Working Paper, Yale University 2014.

_ **and** _ , "Estimating Demand for Solar Photovoltaics," 2017.

Hausman, Jerry A, "Individual discount rates and the purchase and utilization of energy-using durables," *The Bell Journal of Economics*, 1979, pp. 33–54.

Hotz, V Joseph and Robert A Miller, "Conditional choice probabilities and the estimation of dynamic models," *The Review of Economic Studies*, 1993, *60* (3), 497–529.

Hughes, Jonathan E and Molly Podolefsky, "Getting Green with Solar Subsidies: Evidence from the California Solar Initiative," *Journal of the Association of Environmental and Resource Economists*, 2015, *2* (2), 235–275.

Hymes, "Proposed Decision Revising Net Energy Metering Tariffs and Subtariffs," Technical Report, CA State Administrative Law, San Francisco, CA 2022. Online at `https://docs.cpuc.ca.gov/PublishedDocs/Published/G000/M500/K043/500043682.PDF`. Last visited 2022-12-15.

Kind, Peter, "Disruptive Challenges: Financial Implications and Strategic Responses to a Changing Retail Electric Business," Technical Report, Edison Electric Institute 2013.

Kirkpatrick, A. Justin and Lori S. Bennear, "Promoting clean energy investment: An empirical analysis of property assessed clean energy," *Journal of Environmental Economics and Management*, 2014, *68* (2), 357 – 375.

Li, Shanjun, Christopher Timmins, and Roger H von Haefen, "How do gasoline prices affect fleet fuel economy?," *American Economic Journal: Economic Policy*, 2009, *1* (2), 113–137.

Pless, Jacquelyn and Arthur A. van Benthem, "The Surprising Pass-Through of Solar Subsidies," NBER Working Paper 23260, National Bureau of Economic Research, Cambridge, MA March 2016.

Rogers, Evan and Steven Sexton, "Distributed Decisions: The Efficiency of Policy for Rooftop Solar Adoption," Online at https://www.aeaweb.org/conference/2015/retrieve.php?pdfid=844 January 2015.

Appendix Section: Detailed Counterfactual CCP Calculations

The counterfactual change in the probability of adopting, Pr^+, is determined by the change in A plus the change in B:

$$Pr^+ = \Lambda\left(\frac{1}{\sigma}(\delta_1 - \delta_0) + \Delta A + \Delta B\right)$$

We can write B as:

$$\begin{aligned} B &= \rho(log(Pr^{'}) - \gamma) \\ &= \rho\left(\frac{1}{\sigma}(\delta_1^{'} - \delta_0^{'}) + log(1 - Pr')\right) - \rho\gamma \end{aligned}$$

We can write B^+, the value of B under the counterfactual as:

$$\begin{aligned} B^+ &= \rho\left(log(Pr^{'+}) - \gamma\right) \\ &= \rho\left(\frac{1}{\sigma}(\delta_1^{'+} - \delta_0^{'+}) + log(1 - Pr^{'+})\right) - \rho\gamma \end{aligned}$$

Where we denote the counterfactual probability of adopting in the next period as $Pr^{'+}$. Using the fixed progression of VC such that $\Delta A' = \eta\Delta A$, we can write the relationship between counterfactual and observed next-period utility as

$$\frac{1}{\sigma}\left(\delta_1^{'+} - \delta_0^{'+}\right) = \frac{1}{\sigma}\left(\delta_1^{'} - \delta_0^{'}\right) + \overbrace{\Delta A\eta}^{\Delta A'} + \overbrace{\rho(log(Pr^{''+}) - log(Pr^{''}))}^{\Delta B'}$$

We can write the change in B as:

$$
\begin{aligned}
\Delta B &= B^{+} - B \\
&= \rho\left(\frac{1}{\sigma}(\delta_1^{'} - \delta_0^{'}) + \Delta A\eta + \Delta B^{'} + log(1 - Pr^{'+})\right) - \rho\gamma - B \\
&= \rho\left(\frac{1}{\sigma}(\delta_1^{'} - \delta_0^{'}) + \Delta A\eta + \rho(log(Pr^{''+}) - log(Pr^{''})) + log(1 - Pr^{'+})\right) - \rho\gamma \\
&\quad -\rho\left(\frac{1}{\sigma}(\delta_1^{'} - \delta_0^{'}) + log(1 - Pr')\right) - \rho\gamma \\
&= \rho\eta\Delta A + \rho^2(log(Pr^{''+}) - log(Pr^{''})) + \rho(log(1 - Pr^{'+}) - log(1 - Pr^{'})) \\
&= \rho\eta\Delta A + \rho\Delta B^{'} + \rho(log(1 - Pr^{'+}) - log(1 - Pr^{'})) \qquad (29)
\end{aligned}
$$

as shown in equation 20. This can be rewritten using the following recursion:

$$
\begin{aligned}
\Delta B &= \rho\eta\Delta A + \rho(log(1 - Pr^{'+}) - log(1 - Pr^{'})) + \rho\Delta B^{'} \\
&= \rho\eta\Delta A + \rho^2\eta^2\Delta A + \rho\left(log(1 - Pr^{'+}) - log(1 - Pr^{'})\right) + \rho^2\left(log(1 - Pr^{''+}) - log(1 - Pr^{''})\right) + \Delta B^{''} \\
&= \sum_{t=1}^{\infty}\rho^t\eta^t\Delta A + \sum_{s=1}^{\infty}\rho^s\left(log\left(\frac{1 - Pr_s^{'+}}{1 - Pr_s^{'}}\right)\right) \qquad (30)
\end{aligned}
$$